Reactivity tuning of Al/CuO multilayered films by embedding nanoparticles

Baptiste Julien

Reactivity tuning of Al/CuO multilayered films by embedding nanoparticles

Baptiste JULIEN
LAAS-CNRS – 7 Avenue du Colonel Roche, 31031 Toulouse

In this work, gold and silica nanoparticles were added into reactive Al/CuO multilayers systems. Their effects on the flame front dynamics were investigated experimentally using microscopic high-speed imaging technique and theoretically via a reaction model coupling mass and heat diffusion processes. Theoretical findings contradict the experimental observations in which a net increase of the flame front velocity was observed when Au and SiO_2 particles are added in the multilayers. This leads to the conclusion that the faster burn rate observed cannot be fully associated with thermal effects only.

I. INTRODUCTION

Over the past two decades, nanoenergetic materials, especially nanothermites, have received an important interest for additives in propellants, self-propagating high-temperature synthesis (SHS) or pyrotechnic chips[1–9]. Reactive multilayered films (RMFs) consist of stacks composed of alternating thin layers (tens to hundreds of nm) of metal/oxidizer[10–12]. Those thin films are usually deposited using physical vapour deposition (PVD) techniques, such as DC-magnetron sputtering. Multilayers systems offer a stable and reproducible material setting for analysing the different mechanisms involved in reaction process, under external stimulation. Moreover, sputtering deposition technique allows easily controlling the configuration of the multi-layered system, such as layer thickness, stoichiometric ratio or even layering roughness.

Among multilayers, the specific Al/CuO system arouses a lot of interest in applied research, because of its capability of releasing high energy density (~4 $kJ.g^{-1}$), its low ignition temperature and more generally its good reactivity[13–17]. A large part of the research community is dedicated to finding ways to modulate accurately the energetic properties, such as ignition energy[15,18–20] and combustion wave velocity[21,22]. A common way consists in using additives, or dopants (metal, carbons or oxides), without changing the material itself i.e. without changing the nature of reactants, bilayer thickness or equivalence ratio. Despite numerous experimental results, the fundamental mechanisms leading to self-propagating reaction modulation are still unclear, and the comprehension behind the observed results remains evasive.

The purpose of this study is to better understand the effect of additives on the combustion of a thermite system. To reach this goal, highly conductive (Au) and insulator (SiO_2) nanoparticles were embedded in a Al/CuO multilayered systems and the combustion front (flame) is accurately monitored when reaching the Au and SiO2 nanoparticle to analyse locally its effect on the self-propagating combustion. We then confronted the experimental observation with modelling thanks to a 2D combustion model. After the presentations of results, the analysis will be discussed in this paper.

II. Multilayered system and burning experiments

A. Al/CuO multilayered systems

The multilayers system is a well defined system consisting in 15 Al/CuO bilayers, where aluminium layer is 75 nm and copper oxide layer is 150 nm. Giving the well-known thermite reaction ($2Al + 3CuO \rightarrow Al_2O_3 + 3Cu$) this configuration corresponds to a stoichiometric stack. The multilayer were magnetron sputtered on pre-metalized glass substrate, through a physical mask (shadow mask) to pattern a line of nanothermite of 25 mm by 2 mm line (FIG. 1.a). A Ti thin pattern is used to ignite the nanothermite on the left side.

During the process, Au (between 5 and 30 nm) and SiO_2 (150 ± 10 nm) nanoparticles were incorporated into the first CuO layer (FIG

1.b and 1.c). Gold and silica were chosen as their thermal diffusivities are strongly different (127 $mm^2.s^{-1}$ and 1.4 $mm^2.s^{-1}$ respectively). At the end of the process 3 batch of samples were produced: Al/CuO-ref (reference sample without NPs), Al/CuO-SiO_2 and Al/CuO-Au.

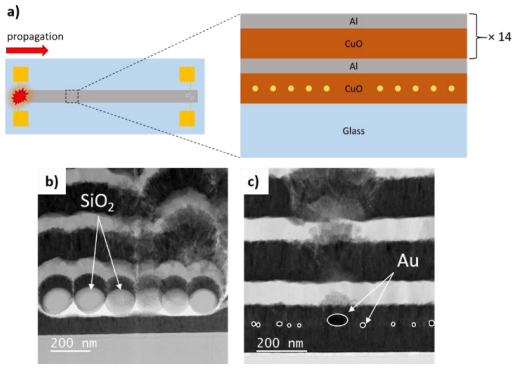

FIG. 1. Front view and cross section schematic of the sample configuration (a). Electronic cross-section of the prepared Al/CuO-SiO_2 (b) and Al/CuO-Au (c) samples.

B. Flame dynamics experimentations

We employed a previously described macro/micro dynamic imaging system[23] to record the nanothermite propagation and probe the combustion front profile. Briefly, the setup consists in a two high-speed cameras system (FIG 2.a), with different time and space imaging resolution. A current pulse (~1 A) is sent through the Ti resistance which by Joule effect ignite the nanothermite.

The top camera enables a macroscopic imaging of the whole propagation (~78µm/pixel, running at 13000 fps). This enable to measure a global flame velocity (global burn rate), defined as the ratio of the total thermite length over the total burn time. The microscopic imaging system employs a second high-speed camera (running at 60000 fps) coupled to a microscopic lens, which enable to reach a space resolution of ~1.7µm/pixel. Thus, the combustion front shape (corrugation) and local point velocity (local burn rate) can be followed with high accuracy. [20]. Both camera were calibrated for color-pyrometry to estimate the flame temperature of the reaction.

From the high speed imaging experiments, we observed that addition of SiO_2 and Au nanoparticles inside the multilayers tends to speed up the reaction front and also increase the flame temperature, compared to the reference sample. Specifically, the global burn rate is measured at 6.1 $m.s^{-1}$ for Au-embedded multi-layered films, which is more than twice the reference Al/CuO films (2.8 $m.s^{-1}$). Furthermore, the average flame temperature is higher (3400 K) compare to reference (2800 K). Silica NPs also affect positively the self-propagating velocity (3.7 $m.s^{-1}$) and so the flame temperature (3000 K), despite the low thermal diffusivity of silicon dioxide. Results are summarized in TAB. 1.

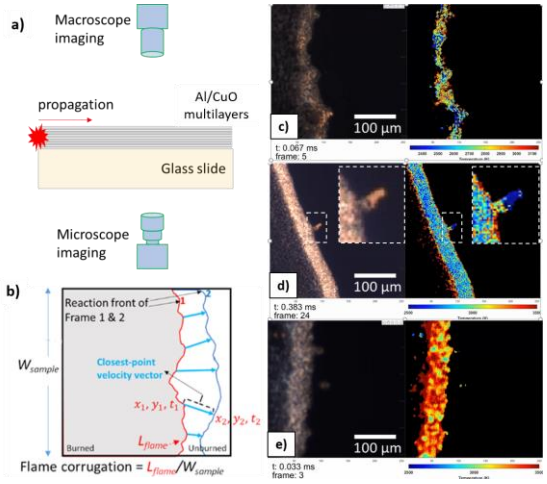

FIG. 2. Experimental configuration for high-resolution pyrometry (a). Schematic showing how micro burn rate is measured (b). Snapshots from raw videos and temperature maps for the reference sample (c), Al/CuO−SiO2 (d) and Al/CuO−Au (e).

	Global burn rate ($m.s^{-1}$)	Local burn rate ($m.s^{-1}$)	Flame temperature (K)
Al/CuO-ref	2.8 ± 0.1	1.9 ± 0.2	2800
Al/CuO-SiO_2	3.7 ± 0.1	2.8 ± 0.1	3000
Al/CuO-Au	6.1 ± 0.1	4.8 ± 0.3	3400

TAB. 1. Front view and cross section schematic of the sample configuration (a). Electronic cross-section of the prepared Al/CuO-SiO_2 (b) and Al/CuO-Au (c) samples.

III. Reaction front modelling of Al-CuO system with embedded particles

In order to better understand the experimental observations we simulated the thermal front propagation across the silica and gold NPs. The model is coupling heat transfer and mass transport, within a 2D meshed geometry. Further details about the model and the equations can be found in previous work[24,25]. This model allows us to tune the volume loading of embedded NPs (number of

particles, size), and calculate the thermal front (reaction front) velocity along the propagation axis. Furthermore, the thermal profile inside the reaction front in the vicinity of NPs can be analysed as further presented.

A. Perturbation of the flame velocity around one single particle

When the reaction front crosses an Au or SiO_2 nanoparticle, a local perturbation of the front velocity is observed (FIG.3). Specifically, silica locally slow down the reaction front by 24 %, while gold object locally speeds up by 20 %. For both case, the combustion front regains its steady state after a pseudo-oscillating regime. Considering the length of the particle (0.13 µm), one can observe the overall perturbation extend well further the particle position.

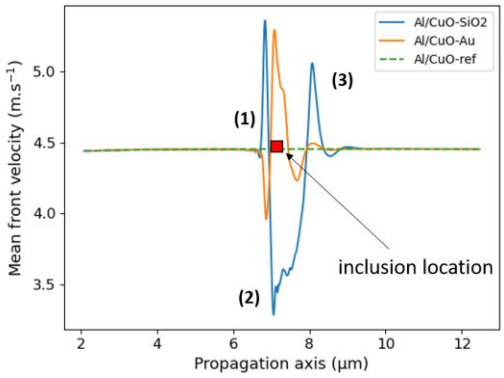

FIG. 3. Evolution of the calculated reaction front velocity along the propagation axis when the combustion front crosses an Au or SiO_2 nanoparticle (indicated by red square).

B. Influence of the particle loading on the flame velocity

In order to better imitate the experiments, we performed simulations with multiple nanoparticles inside the thermite system: 1, 7, 14 and 20 NPs, which corresponds to different volume loadings (in vol. %). The global front velocity, defined as the velocity averaged along the overall propagation length is plotted in the FIG. 4 in terms of velocity changes as a function of the volume loading. The results show that the averaged flame velocity changes linearly when increasing the particle loading, but with opposite trends. Specifically, the higher thermal diffusivity of Au results in a limited flame velocity increase while the silica NPs has a more dramatic effect: flame velocity drops by 17%.

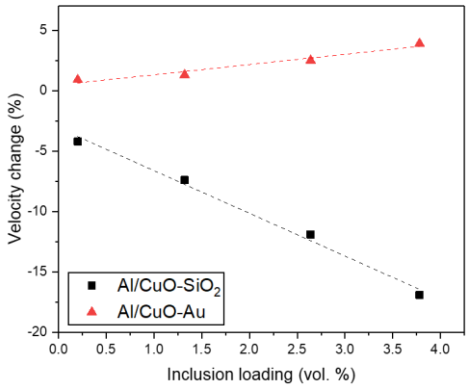

FIG. 4. Relative change (in % relatively to the reference system at 4.45 $m.s^{-1}$) of the self-propagating velocity (global burn rate) for different NPs loadings (in vol. %)

IV. CONCLUSION

This work concluded conflicting results between experimental observations and theoretical results. Combustion experiments showed an enhancement of the flame velocity in multilayers containing Au and SiO_2 NPs in their first bilayer. Whereas 2D propagation model predicts a slowdown of the flame especially when silica NPs. This result leads to the conclusion that the faster experimental combustion velocity observed with additives cannot be fully associated to thermal effects. Instead we propose that other chemically and/or mechanically based processes must play a role in the enhancement of the reaction rate. We suggest that locally, i.e. at the vicinity of additives, high stressed zone are created during the flame front crossing because of extreme temperature gradient associated with radically different thermal expansion coefficient differences between NPs and thermites. This assumption needs to be looked to further in a future study.

References

[1] K.S. Martirosyan, L. Wang, A. Vicent, and D. Luss, Prop., Explos., Pyrotech. NA (2009).
[2] C. Rossi, *Al-Based Energetic Nano Materials* (n.d.).
[3] E.R. Westphal, A.K. Murray, M.P. McConnell, T.J. Fleck, G.T. -C. Chiu, J.F. Rhoads, I.E. Gunduz, and S.F. Son, Prop., Explos., Pyrotech. **44**, 47 (2019).
[4] C.S. Staley, K.E. Raymond, R. Thiruvengadathan, S.J. Apperson, K.

Gangopadhyay, S.M. Swaszek, R.J. Taylor, and S. Gangopadhyay, Journal of Propulsion and Power **29**, 1400 (2013).
[5] A. Bezmelnitsyn, R. Thiruvengadathan, S. Barizuddin, D. Tappmeyer, S. Apperson, K. Gangopadhyay, S. Gangopadhyay, P. Redner, M. Donadio, D. Kapoor, and S. Nicolich, Propellants, Explosives, Pyrotechnics **35**, 384 (2010).
[6] H. Pezous, C. Rossi, M. Sanchez, F. Mathieu, X. Dollat, S. Charlot, and V. Conédéra, Journal of Physics and Chemistry of Solids **71**, 75 (2010).
[7] C. Rossi, B. Larangot, P. Pham, D. Briand, N.F. de Rooij, M. Puig-Vidal, and J. Samitier, Journal of Microelectromechanical Systems **15**, 1805 (2006).
[8] A. Chaalane, C. Rossi, and D. Estève, Sensors and Actuators A: Physical **138**, 161 (2007).
[9] G.A.A. Rodríguez, S. Suhard, C. Rossi, D. Estève, P. Fau, S. Sabo-Etienne, A.F. Mingotaud, M. Mauzac, and B. Chaudret, J. Micromech. Microeng. **19**, 015006 (2008).
[10] C. Rossi, Prop., Explos., Pyrotech. **44**, 94 (2019).
[11] D.P. Adams, Thin Solid Films **576**, 98 (2015).
[12] M.L. Hitchman, Chemical Vapor Deposition **3**, 144 (1997).
[13] L. Marín, C.E. Nanayakkara, J.-F. Veyan, B. Warot-Fonrose, S. Joulie, A. Estève, C. Tenailleau, Y.J. Chabal, and C. Rossi, ACS Appl. Mater. Interfaces **7**, 11713 (2015).
[14] L. Marín, Y. Gao, M. Vallet, I. Abdallah, B. Warot-Fonrose, C. Tenailleau, A.T. Lucero, J. Kim, A. Esteve, Y.J. Chabal, and C. Rossi, Langmuir **33**, 11086 (2017).
[15] A. Nicollet, G. Lahiner, A. Belisario, S. Souleille, M. Djafari-Rouhani, A. Estève, and C. Rossi, Journal of Applied Physics **121**, 034503 (2017).
[16] P. Zhu, R. Shen, Y. Ye, S. Fu, and D. Li, Journal of Applied Physics **113**, 184505 (2013).
[17] C. Wang, J. Xu, Y. Shen, Y. Wang, T. Yang, Z. Zhang, F. Li, R. Shen, and Y. Ye, Defence Technology (2020).
[18] G. Lahiner, A. Nicollet, J. Zapata, L. Marín, N. Richard, M.D. Rouhani, C. Rossi, and A. Estève, Journal of Applied Physics **122**, 155105 (2017).
[19] Z. Qiao, J. Shen, J. Wang, B. Huang, Z. Yang, G. Yang, and K. Zhang, Composites Science and Technology **107**, 113 (2015).
[20] H. Wang, B. Julien, D.J. Kline, Z. Alibay, M.C. Rehwoldt, C. Rossi, and M.R. Zachariah, J. Phys. Chem. C **124**, 13679 (2020).
[21] J. Zapata, A. Nicollet, B. Julien, G. Lahiner, A. Esteve, and C. Rossi, Combustion and Flame **205**, 389 (2019).
[22] I. Abdallah, J. Zapata, G. Lahiner, B. Warot-Fonrose, J. Cure, Y. Chabal, A. Esteve, and C. Rossi, ACS Appl. Energy Mater. **1**, 1762 (2018).
[23] H. Wang, D.J. Kline, and M.R. Zachariah, Nat Commun **10**, 1 (2019).
[24] B. Julien, H. Wang, E. Tichtchenko, S. Pelloquin, A. Esteve, M.R. Zachariah, and C. Rossi, Nanotechnology **32**, 215401 (2021).
[25] E. Tichtchenko, A. Estève, and C. Rossi, Combustion and Flame **228**, 173 (2021).